Biophysical Chemistry 22 (1985) 131–143
Elsevier

BPC 00929

NANOSECOND DYNAMICS OF CHARGED FLUORESCENT PROBES AT THE POLAR INTERFACE OF A MEMBRANE PHOSPHOLIPID BILAYER

Alexander P. DEMCHENKO and Nina V. SHCHERBATSKA

The Palladin Institute of Biochemistry, Academy of Sciences of the Ukrainian SSR, 252030 Kiev, U.S.S.R.

Received 25th July 1984
Revised manuscript received 13th February 1985
Accepted 21st February 1985

Key words: Phospholipid membrane; Amphiphilic molecule; Fluorescent probe; Red-edge excitation fluorescence shift; Time-resolved spectroscopy; Subnanosecond mobility; Nanosecond mobility

Molecular relaxation fluorescence methods were applied to analyze the nature and characteristic times of motions of amphiphilic molecules absorbed in the polar region of a phospholipid bilayer. The fluorescence probes 2-toluidinonaphthalene-6-sulfonate and 1-anilinonaphthalene-8-sulfonate in egg phosphatidylcholine vesicles were studied. The methods of edge excitation fluorescence red shifts, nanosecond time-resolved spectroscopy, fluorescence quenching by hydrophilic and hydrophobic quenchers and emission wavelength dependence of polarization were used. The structural (dipolar) relaxation is shown to be a very rapid (subnanosecond) process. The observed nanosecond phenomena are related to translational movement of the chromophore itself towards a more polar environment and its rotation. The polar surface area of the phospholipid membrane appears to be a highly mobile liquid-like system.

1. Introduction

One of the important features of membrane phospholipid bilayers that determine their absorption and transport properties is the polarity gradient formed by the oriented phospholipid molecules. The non-polar central area, the glycerol backbone area that contains polarizable carbonyl groups as well as the surface area which is formed by the charged phospholipid heads, bound water and adsorbed ions, may be distinguished. The interaction of different molecules with the membrane and changes of its properties depend greatly on the depth of their location.

The most important appear to be the structural dynamic properties of the surface polar area. The substances producing a significant influence on the membrane structure, e.g., detergents, local anesthetics and other amphiphiles, are bound in this area. Many of the metabolites and substances with physiologic activity are amphiphilic. The question arises about the ranges of space and time within which the motions of both adsorbed molecules and the phospholipid groups interacting with them exist. Which are the stages, mechanisms, and the speed of reaching energetic equilibrium in these systems?

Among the amphiphilic molecules located in the surface polar area of membranes studied are the aminonaphthalenesulfonates, especially 1,8-ANS and 2,6-TNS which are widely used as fluorescence probes [1–3]. Their distribution coefficient between water and hydrophobic solvent is close to unity [4], but they are bound by phospholipid bilayers with a high association constant, of the order of 10^{-4}–10^{5} M^{-1} and may reach significant saturation – 1 molecule per 6–10 phospholipid molecules [5–7]. The binding does not change the bilayer properties, and the distances

Abbreviations: 1,8-ANS, 1-anilinonaphthalene-8-sulfonate; 2,6-TNS, 2-toluidinonaphthalene-6-sulfonate.

and interactions between the phospholipid molecules significantly [3,6].

There are many publications on 1,8-ANS and 2,6-TNS fluorescence in membranes [2,3,8]. However, the methods of steady-state spectroscopy used did not allow the direct analysis of structural dynamics. Brand et al. [9–12] were the first to apply nanosecond time-resolved spectroscopy and show the nanosecond kinetics of 2,6-TNS fluorescence spectra that reveal some relaxation process in this time range. The nanosecond motions of spectra were also observed by oxygen quenching lifetime-resolved spectra [13] and phase fluorimetry [14]. Nevertheless, the character of movements in space and time has not been determined. Dielectric relaxation [15] and NMR studies [16–18] demonstrate the fast subnanosecond and nanosecond dynamics of dipolar groups in the bilayer.

In the present study the analysis of static and dynamic inhomogeneous broadening of the spectra based on edge excitation fluorescence effects, which was developed earlier in the studies of protein [19,20], has been used to investigate structural mobility in the phospholipid bilayer. Time-resolved spectroscopy is also applied along with studies of the emission wavelength dependence of steady-state polarization. Fluorescence studies of 2,6-TNS and 1,8-ANS in phospholipid vesicles are performed under the influence of hydrophilic and hydrophobic quenchers. The results suggest the existence of two different processes: subnanosecond structural (dipolar) relaxation and nanosecond changes of probe position and orientation.

2. Materials and methods

The studies were performed on vesicles from egg yolk phosphatidylcholine obtained by a conventional method [21]. Vesicles were formed by short-term (10–15 min) sonication of the lipid suspension in 50 mM Tris-HCl buffer, pH 7.4, using a 150-W ultrasonic disintegrator (MSE). The lipid concentration was 10 mg/ml and the volume 2–3 ml. Under these conditions, small single-bilayer vesicles are predominantly formed. The 1,8-ANS and 2,6-TNS solutions in water were added to the sonicated lipid suspension to a final probe : phospholipid molar ratio of 1 : 100 which is significantly (by an order) lower than their saturating concentration [5,6]. All fluorescence quenchers, excluding ferrocene (dicyclopentadienyliron), were added to the liposome suspension from aqueous solutions. Ferrocene was added to the phospholipid solution in chloroform/methanol solvent prior to drying and suspending in aqueous buffer.

1,8-ANS and 2,6-TNS were obtained from Serva (F.R.G.). Fluorescein, rhodamine 6G and eosin of chromatographic purity were dyes produced in the U.S.S.R. Ferrocene was of reagent grade.

Measurements of absorption spectra and spectrophotometric determinations of concentration were performed on a Specord M 40 spectrophotometer (Carl Zeiss, G.D.R.).

Fluorescence spectra were recorded on an MPF-4 spectrophotometer (Hitachi, Japan) in the ratio-recording mode, excitation and emission slits being 2–5 nm. The background spectra (of the probe-free liposome suspension with or without quenchers) were recorded and subtracted. The spectra of 1,8-ANS and 2,6-TNS in ethanol and water were in agreement with published data [22,23]. The correction for spectral sensitivity, therefore, was not performed. In order to exclude light-scattering artefacts, fluorescence was recorded from the surface of a thin (1 mm) quartz cell. The cell was thermostatted by circulating water or an ethanol/water mixture using an MK-70 cryothermostat (G.D.R.).

Polarization measurements were performed using a Hitachi polarization accessory with polaroid films. The results were corrected for the instrumental factor by a conventional method [24].

The nanosecond fluorescence decay curves and time-resolved emission spectra were recorded on a PRA System 3000 fluorescence lifetime instrumentation (Photochemical Research Associates Inc., Canada). A 510 C nanosecond excitation lamp with a pulse width of 2 ns and a repetition rate of 50 kHz was used. The excitation and emission monochromators were model 1200 holographic grating monochromators, and the spectral bandwidth 16 nm. The detection system was based on the time-correlated single-photon-counting technique. The standard block of programs was supplied by the instrument manufacturers. No

polarizers were used in decay measurements. To evaluate the functional form of the undistorted fluorescence decay, a linearized least-squares reconvolution technique was used. The decay kinetics was expressed as a sum of two components:

$$I(t) = A_1 \exp(-t/\tau_1) + A_2 \exp(-t/\tau_2) \qquad (1)$$

Time-resolved emission spectra were determined using the lower and upper level discriminators of the multichannel analyzer (MCA) for selection of a portion of the fluorescence decay curve. With the MCA operating in the multichannel sealing mode it was swept together with the emission monochromators and the resultant spectrum was stored in the memory.

3. Results

3.1. Edge-excitation fluorescence effects in the steady-state spectra

The fluorescence spectra of aromatic molecules in solution are known to be inhomogeneously broadened due to the statistical distribution of interaction energy between chromophores and the surrounding molecules and groups of atoms [25–28]. The effects of inhomogeneous broadening depend essentially on the correlation between the excitation lifetime τ_F and structural (dipolar) relaxation time τ_R^{dip}. In liquid solvents the fast structural redistributions in solvates with different energy do not allow one to observe the spectral effects originating from their photoselection (dynamic inhomogeneous broadening). In the case $\tau_R^{dip} \geqslant \tau_F$ (i.e., solid and viscous solvents), such redistributions do not have sufficient time to reach completion and the effects of static inhomogeneous broadening of spectra may be observed. One of these effects is the long-wave shift of fluorescence spectra at the long-wave edge excitation [25,26]. The method of analysis of nanosecond structural relaxation is based on this phenomenon [19,20]: in the case when a fast subnanosecond relaxation exists, the above effect is absent, and if it is slow enough not to proceed during the excited state lifetime, the effect is maximal.

The dependence of the position of the maxima of fluorescence spectra λ_F(max) for 2,6-TNS on the excitation wavelength for solid, viscous and liquid systems is presented in fig. 1. In ethanol at 20°C the edge excitation fluorescence shift is not observed (as is the case with other liquid solvents tested earlier [19]). The shift is very small in glycerol at 35°C. But, on transition to viscous glycerol (at 1°C) and further to solid glycerol (at −15°C), the effect increases significantly reaching 25–30 nm and above.

The results on 2,6-TNS in egg phosphatidylcholine vesicles show no changes of fluorescence spectra on transition to edge excitation (fig. 1). This is similar to probe behavior in liquid solvents and demonstrates the existence of fast subnanosecond mobility of molecules or atom groups in the environment of the electronically excited chromophore. In other words, the polar area of a phospholipid bilayer, where the probe is located, appears to be a highly mobile liquid system.

Similar behavior is observed for 1,8-ANS. There is a significant edge excitation red shift observed in solid and viscous solvents, reaching 20 nm and greater. However, in phosphatidylcholine vesicles the fluorescence spectrum is observed at 480 nm

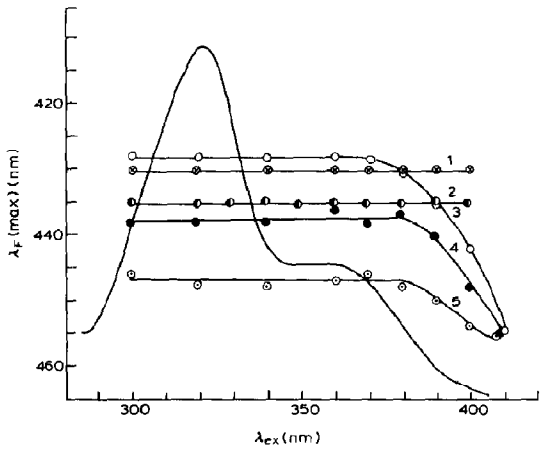

Fig. 1. The dependence of the maxima of the fluorescence spectra λ_F(max) of 2,6-TNS on the excitation wavelength λ_{ex}. (1) In ethanol, $t = 20$°C; (2) in phosphatidylcholine vesicles, $t = 20$°C; (3) in glycerol, $t = -15$°C; (4) in glycerol, $t = 1$°C; (5) in glycerol, $t = 35$°C. Solid line, excitation spectrum.

and does not depend on excitation wavelength, including the long-wave excitation at 380–430 nm.

3.2. Nanosecond time-resolved spectroscopy

The kinetic processes proceeding at times comparable with τ_F are analyzed by two approaches to kinetic spectroscopic data [9–12,29]: (1) The wavelength dependence of the fluorescence emission decay. In the case of a nanosecond change of the chromophore emission properties, apparent non-exponential decay (appearance of a fact component) is observed at the short-wave edge of the emission spectrum and the fluorescence temporal increase (negative component) followed by exponential decay is seen at the far long-wave emission. (2) The direct observation of temporal shifts in the nanosecond time-resolved spectra.

Both of these approaches were used in studies of phosphatidylcholine vesicles. The results show the temporal long-wave shift of 2,6-TNS and 1,8-ANS spectra (fig. 2). A characteristic change of the decay curves over the fluorescence spectrum is also observed (fig. 3). These results are in agreement with the data of Brand et al. [9–12] obtained

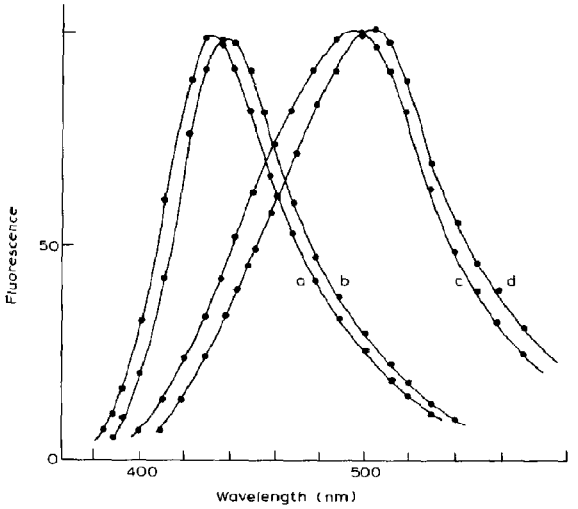

Fig. 2. The nanosecond time-resolved spectra of 2,6-TNS (a,b) and 1,8-ANS (c,d) in phosphatidylcholine vesicles at 3 ns (a,c) and 35 ns (b,d) after excitation. The time window is 10 channels (3.2 ns). Temperature, 20°C.

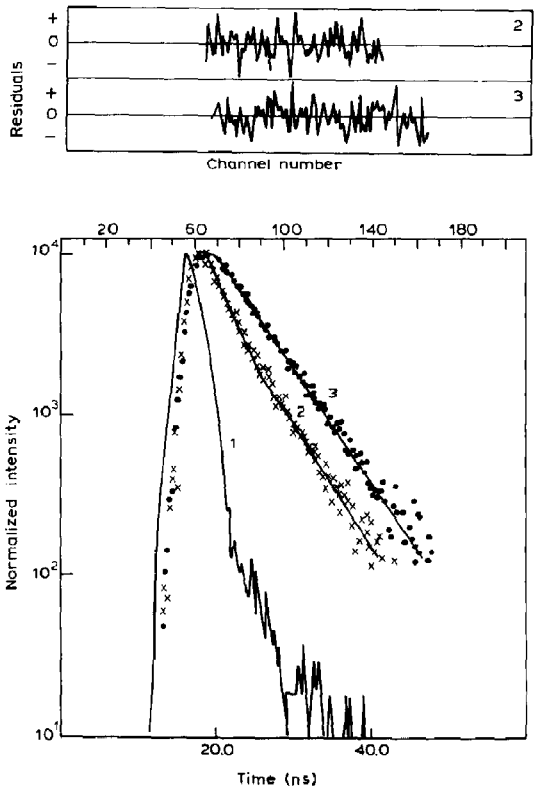

Fig. 3. The decay curves of 2,6-TNS in phosphatidylcholine vesicles. Excitation wavelength, 360 nm; emission wavelength, 400 nm (×) and 480 nm (○). Solid curves: (1) an experimental lamp profile, (2,3) the best-fit approximation curves. CHISQ = 1.051 for curve 2, CHISQ = 0.937 for curve 3. Temperature, 20°C.

earlier on phosphatidylcholine vesicles. They studied this phenomenon in detail and showed the nanosecond spectral effects to result from the excited-state process in the nanosecond time range, rather than from the heterogeneous emission of probe molecules located at different sites.

The process of relaxation is not adequately described by two-component exponential decay curves [10], while the two-component decay analysis allows one to follow the nanosecond kinetics easily and to analyse it on an empirical basis. The short-lived component is essential at the short-wave emission. It decreases at the maximum of the fluorescence spectrum and disappears at the long-

Table 1

Two-exponential analysis of 2,6-TNS and 1,8-ANS fluorescence decay data in egg phosphatidylcholine vesicles at different emission wavelengths (λ_{em})

Excitation at 360 nm (2,6-TNS) and 380 nm (1,8-ANS). Temperature, 20°C.

λ_{em} (nm)	A_1	τ_1 (ns)	A_2	τ_2 (ns)	I_1/I_2 [a]
2,6-TNS					
400	0.59 (±0.06)	1.39 (±0.18)	0.20 (±0.01)	6.29 (±0.19)	0.39
430	0.29 (±0.02)	2.45 (±0.57)	0.32 (±0.03)	6.85 (±0.21)	0.18
480	−1.22 (±0.52)	0.12 (±0.06)	0.40 (±0.01)	6.59 (±0.05)	0.03
500 [b]	–	–	0.80 (±0.01)	6.53 (±0.03)	0
1,8-ANS					
440	0.36 (±0.04)	1.61 (±0.24)	0.28 (±0.01)	8.17 (±0.16)	0.20
470	0.20 (±0.02)	2.77 (±0.58)	0.41 (±0.02)	8.18 (±0.21)	0.14
520 [b]	–	–	0.41 (±0.05)	8.02 (±0.06)	0

[a] Ratio of integral intensities of the components.
[b] A single-component analysis was performed.

wave edge of the emission spectrum, where a short-lived negative component (temporal increase of intensity) may be observed [9]. The two-exponential analysis of the decay curves is presented in table 1. For 2,6-TNS these results are in reasonable agreement with the data presented by others [9]. The decreased τ_F at the short-wave emission was also observed by phase and modulation lifetime techniques [14]. The data presented in table 1 show the close similarity between the behavior of 2,6-TNS and 1,8-ANS, probes that differ in electronic structure, but have similar τ_F values.

In previous works nanosecond excited-state processes were related to the dipolar structural relaxation proceeding in the nanosecond time range [9–14]. However, the data presented above on the absence of edge excitation fluorescence shifts demonstrate the completeness of dipolar relaxation prior to emission. Information on the rate of the dipolar relaxation may be obtained from time-resolved spectroscopic data as follows. If the dipolar relaxational equilibrium is established prior to emission, the emission decay does not depend on the excitation wavelength. If the dipolar relaxation proceeds simultaneously with the emission, the red-edge excitation selects the chromophores, the energy of which corresponds more closely to the relaxed state [27]. Their emission spectra are already red-shifted and an altered decay kinetics may be observed. Indeed, for 2,6-TNS in glycerol (table 2) and red-edge excitation reduces the short-lived component (positive at the short-wave edge and negative at the long-wave edge) of the decay curves. For 2,6-TNS in phosphatidylcholine vesicles no effect of red edge exitation is observed (table 3).

Table 2

Two-exponential analysis of 2,6-TNS fluorescence decay data at different excitation (λ_{ex}) and emission (λ_{em}) wavelengths in glycerol at 10°C

2,6-TNS concentration, 2×10^{-4} M.

λ_{em} (nm)	λ_{ex} (nm)	A_1	τ_1 (ns)	A_2	τ_2 (ns)	I_1/I_2
430	360	0.50 (±0.02)	2.09 (±0.15)	0.27 (±0.02)	6.47 (±0.20)	0.37
	390	0.47 (±0.03)	1.86 (±0.18)	0.31 (±0.02)	6.63 (±0.14)	0.30
490	360	−0.93 (±0.07)	0.38 (±0.04)	0.69 (±0.01)	6.44 (±0.03)	0.07
	390 [a]	–	–	0.56 (±0.04)	6.43 (±0.03)	0

[a] A single-component analysis was performed.

Table 3

Two-exponential analysis of 2,6-TNS fluorescence decay data at different excitation (λ_{ex}) and emission (λ_{em}) wavelengths in egg phosphatidylcholine vesicle at 25°C

λ_{em} (nm)	λ_{ex} (nm)	A_1	τ_1 (ns)	A_2	τ_2 (ns)	I_1/I_2
430	360	0.43 (±0.03)	1.56 (±0.16)	0.43 (±0.02)	5.98 (±0.09)	20.5
	390	0.39 (±0.03)	1.79 (±0.22)	0.45 (±0.02)	5.98 (±0.09)	20.8
500	360 [a]	-	-	0.76 (±0.01)	5.72 (±0.04)	0
	390 [a]	-	-	0.76 (±0.01)	5.69 (±0.04)	0

[a] A single-component analysis was performed.

The differences in probe behavior in viscous glycerol solution and in phospholipid vesicles may also be found in the data presented by others. DeToma et al. [10] observed differences in the temporal changes of bandwidth of fluorescence spectra. In the case of dipolar relaxation in the course of emission, as well as in the case of steady-state spectra on transition from solid to liquid solvent [30,31], the minimal width should be observed for unrelaxed states (solid solutions or early periods of time), a greater width for the relaxed states (liquid solutions or late periods of time), and the maximal width for the intermediate case, where chromophores at different stages of relaxation participate in emission. Such a dependence was observed in glycerol [10], but in phospholipid vesicles the bandwidth in the course of emission remained unchanged.

3.3. Fluorescence quenching by water-soluble and lipid-soluble fluorescence quenchers

The location of 1,8-ANS and 2,6-TNS molecules at the polar interface of a phospholipid bilayer suggests the possibility of fluorescence quenching at the dynamic contacts with both water-soluble and non-polar quenchers that may be dissolved in the hydrophobic central area of the bilayer. In the case when the probe location is not changed at time τ_F, similar influences on chromophore emission of differently located quenchers may be expected. If the probe location is changed simultaneously with the emission, differences in the quenching effect from the inside and outside of the bilayer may be expected.

The concentration ranges and Stern-Volmer quenching constants of the quenchers are presented in table 4. The mechanism of quenching is paramagnetic for ferrocene and excited-state energy transfer for other quenchers. It is essential that in both cases the quenching is dynamic, producing the decrease in fluorescence lifetime. The observed linearity of Stern-Volmer plots does not prove the diffusional mechanism of quenching. Rather, the high values of the quenching constants suggest the water-soluble quenchers to be associated with the bilayer surface.

Table 4

Stern-Volmer quenching constants (K_{SV}) for 2,6-TNS and 1,8-ANS in egg phosphatidylcholine vesicles by different water-soluble quenchers at 20°C

Quencher	Concentration range (M)	K_{SV}
2,6-TNS		
Rhodamine 6G	3.7×10^{-5}–6.0×10^{-5}	1.4×10^{4}
Fluorescein	1.0×10^{-7}–1.0×10^{-5}	1.7×10^{5}
Eosin	1.0×10^{-5}–1.0×10^{-4}	1.5×10^{4}
1,8-ANS		
Rhodamine 6G	1.0×10^{-6}–1.0×10^{-5}	1.8×10^{5}
Eosin	1.0×10^{-6}–1.0×10^{-4}	1.0×10^{5}

Table 5

The influence of quenchers on the emission properties of 2,6-TNS and 1,8-ANS in egg phosphatidylcholine vesicles at 30°C.

Quencher	Concentration (mol/l)	Wavelength of fluorescence maxima (nm)		Polarization
		Mean excitation [a]	Edge excitation [b]	
2,6-TNS				
None	–	435	435	0.23
Rhodamine 6G	5.7×10^{-5}	431	431	0.30
Eosin	4.75×10^{-5}	431	431	0.30
Fluorescein	1.4×10^{-5}	432	432	0.27
Ferrocene	3.3×10^{-5}	435	435	–
1,8-ANS				
None	–	480	480	0.22
Rhodamine 6G	5.8×10^{-5}	475	475	0.27
Eosin	2.6×10^{-4}	475	475	0.27
Fluorescein	2.7×10^{-5}	470	470	–
Ferrocene	2.8×10^{-5}	480	480	–

[a] Excitation at 360 nm for 2,6-TNS and 380 nm for 1,8-ANS.
[b] Excitation at 400 nm for 2,6-TNS and 430 nm for 1,8-ANS.

The results on 2,6-TNS fluorescence quenching by different concentrations of rhodamine 6G in phospholipid vesicles are presented in fig. 4. The 40 and 70% quenchings result in a short-wave shift by 3 and 5 nm, respectively. Other water-soluble quenchers fluorescein and eosin were tested and found to quench the emission of 2,6-TNS and 1,8-ANS in vesicles (table 5), in all cases a clear short-wave shift being observed.

In contrast, the hydrophobic quencher ferrocene in concentrations producing a similar quenching effect does not produce any significant shift of the emission of both 1,8-ANS and 2,6-TNS (table 5 and fig 5).

It may be suggested that rhodamine 6G and other water-soluble quenchers predominantly quench the long-wave emitting relaxed species. The results of the two-exponential analysis of the decay curves (table 6) show that for rhodamine 6G only the lifetime of the long-lived component of emission is reduced. For ferrocene both components are reduced, the most significant being the decrease in the lifetime of the short-lived component.

The selectivity of quenching of the 'late' emission also follows from the comparison of our data with the results of Lakowicz and Hogen [13] on 2,6-TNS in vesicles on quenching by oxygen. Oxygen may be dissolved in both polar and non-

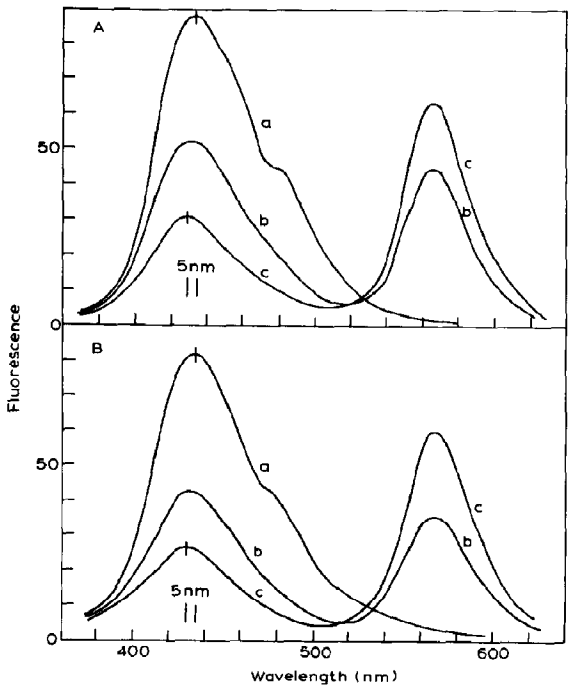

Fig. 4. The results on 2,6-TNS fluorescence quenching by rhodamine 6G in phosphatidylcholine vesicles. Excitation wavelengths: 360 nm (A) and 390 nm (B). (a) Without quencher, (b) 4×10^{-5} M, (c) 6×10^{-5} M.

Table 6

Two-exponential analysis of the influence of quenchers on 2,6-TNS and 1,8-ANS fluorescence decay kinetics in egg phosphatidylcholine vesicles

Excitation at 360 nm for 2,6-TNS and 380 nm for 1,8-ANS. Emission at 435 nm for 2,6-TNS and 470 nm for 1,8-ANS. Temperature, 20°C.

Quencher	Concentration (mol/l)	A_1	τ_1 (ns)	A_2	τ_2 (ns)	I_1/I_2
2,6-TNS						
None	-	0.20 (±0.02)	2.45 (±0.57)	0.32 (±0.03)	6.85 (±0.21)	0.18
Rhodamine 6G	4.8×10^{-5}	0.28 (±0.02)	2.01 (±0.36)	0.23 (±0.03)	5.94 (±0.24)	0.29
Ferrocene	1.0×10^{-4}	0.40 (±0.02)	1.69 (±0.19)	0.46 (±0.02)	5.74 (±0.11)	0.20
1,8-ANS						
None	-	0.20 (±0.02)	2.77 (±0.58)	0.41 (±0.02)	8.18 (±0.21)	0.14
Rhodamine 6G	3.4×10^{-5}	0.26 (±0.02)	3.10 (±0.41)	0.19 (±0.03)	7.66 (±0.40)	0.35
Ferrocene	1.0×10^{-4}	0.13 (±0.04)	1.44 (±0.64)	0.19 (±0.01)	5.45 (±0.16)	0.16

polar media, and quenching as high as 10-fold is required to observe shifts by several nanometers.

The selective quenching of the relaxed component may be due to its better overlap integral of the fluorescence spectrum with the absorption spectrum of the quencher. If so, the effect would depend on the absorption spectrum of the acceptor, which is not the case. In the case of fluorescein ($\lambda_{max} = 480$ nm), rhodamine 6G ($\lambda_{max} = 527$ nm) and eosin ($\lambda_{max} = 532$ nm) similar shifts are observed for both 2,6-TNS and 1,8-ANS.

Another possibility for the selective quenching of the late states which appears to be more probable is the translational motion of the probe along the polarity gradient out of the membrane. As a result, the polar quencher approaches the probe more closely, thus decreasing the excitation-energy transfer distances. No other reaction in the excited state could explain such time-dependent quenching.

The influence of quenchers on the fluorescence spectra at the mean (360 nm) and red-edge (390 nm) excitations may be compared. Both water-soluble (fig. 4) and hydrophobic (fig. 5) quenchers produce no excitation wavelength-dependent differences. Thus, the edge excitation fluorescence red shift is absent when τ_F decreases as a result of quenching. The dipolar-orientational equilibrium was established at the time prior to emission. An additional argument in favor of this conclusion is the equal intensity of sensitized rhodamine 6G fluorescence observed at 563 nm at the mean and red-edge excitation wavelengths of 2,6-TNS. In case the dipolar relaxation does not have time to occur, the excitation-energy transfer efficiency would depend on λ_{ex}: the spectra are inhomogeneously broadened and at the red-edge excitation the photoselection of a chromophore subpopulation with a better overlap integral of the fluorescence spectra with the absorption spectra of the acceptor would become possible [31].

3.4. *Fluorescence polarization*

The polarization of chromophore emission reflects the ability of a chromophore to rotate over a time period comparable with the excited-state lifetime. The limiting polarization values (P_0) for 1,8-ANS and 2,6-TNS in viscous and solid solvents are 0.4–0.46 [22,33]. In phosphatidylcholine vesicles much smaller polarization (P) values (0.15–0.27) were observed [3,8]. The results presented in fig. 6 show the significant dependence of 2,6-TNS polarization on temperature: it increases with decreasing temperature. The experiments at $t \leqslant 0$°C were performed in 20% sucrose. At 0°C the results with and without sucrose were identical. In viscous sucrose solution the rotation of vesicles is slowed down, and the decreased polarization, therefore, should be attributed to the rotation of the probe itself with respect to the bilayer plane.

The fluorescence polarization of an isotropi-

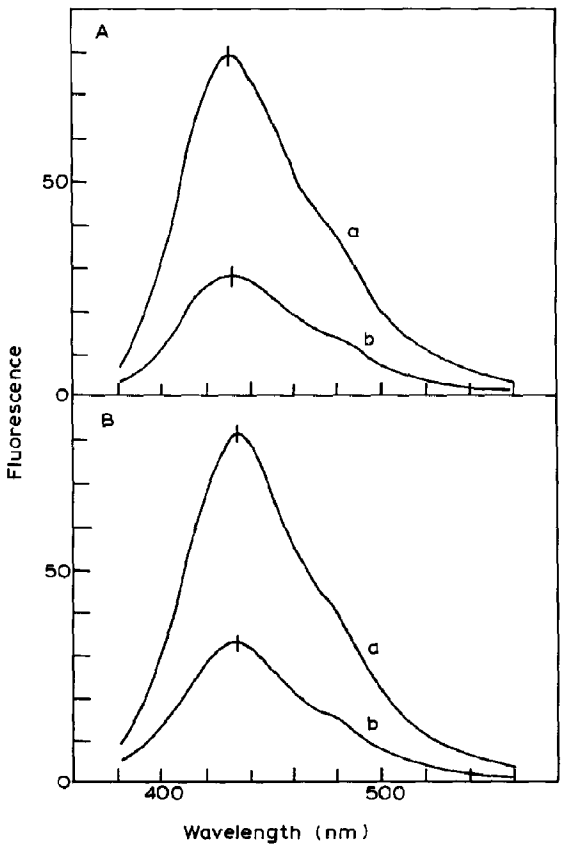

Fig. 5. The results on 2,6-TNS fluorescence quenching by ferrocene in phosphatidylcholine vesicles. Excitation wavelengths: 360 nm (A) and 390 nm (B). (a) Without quencher; (b) 10^{-4} M.

cally rotational chromophore in viscous solution depends on temperature and fluorescence lifetime according to the Perrin equation:

$$\frac{r_0}{r} = 1 + \frac{kT}{\eta V}\tau_F \qquad (1)$$

where r is the steady-state emission anisotropy, which correlates with polarization ($r = 2P/(3 - P)$), and r_0 the limiting anisotropy in the absence of chromophore rotation. The rotational relaxation time $\tau_R^{rot} = V\eta/kT$ depends on the volume of the chromophore molecule and is inversely proportional to the ratio of the temperature (on the absolute scale) T to the medium viscosity η. Fluorescence quenchers decreasing τ_F significantly increase the polarization of 2,6-TNS and 1,8-ANS emission (table 5).

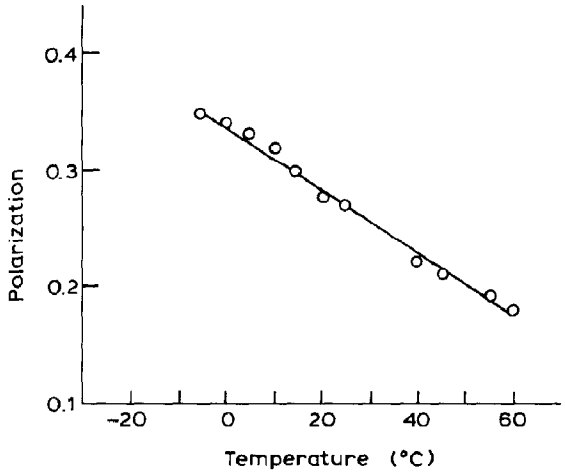

Fig. 6. The dependence of 2,6-TNS fluorescence polarization in phosphatidylcholine vesicles on temperature. Excitation, 360 nm; emission, 430 nm.

As a result of the nanosecond movement of spectra τ_F differs along the emission spectrum. If the temporal shift of the spectra and chromophore rotation is in the same time range, the emission at different wavelengths should be polarized differently [29,31]. Fig. 7 presents the dependence of polarization on the emission wavelength for 2,6-TNS with and without fluorescence quenchers. The lowest polarization is observed at the long-wave edge where the relaxed late emission is dominant. With decrease in emission wavelength the participation of short-lived 'early' emission increases, resulting in the observed increase of polarization. The results are in qualitative agreement with theory relating the emission decay function $I(\lambda_{em}, t)$ and τ_R^{rot} with anisotropy at emission wavelength λ_{em} [29]:

$$r(\lambda_{em}) = \frac{r_0 \int_0^\infty I(\lambda_{em}, t) \exp(-t/\tau_R^{rot}) dt}{\int_0^\infty I(\lambda_{em}, t) dt} \qquad (2)$$

Though the chromophore rotations are thought to be anisotropic eqs. 1 and 2, which are valid for isotropic rotational motions only, present a qualitatively good description of the observed effects.

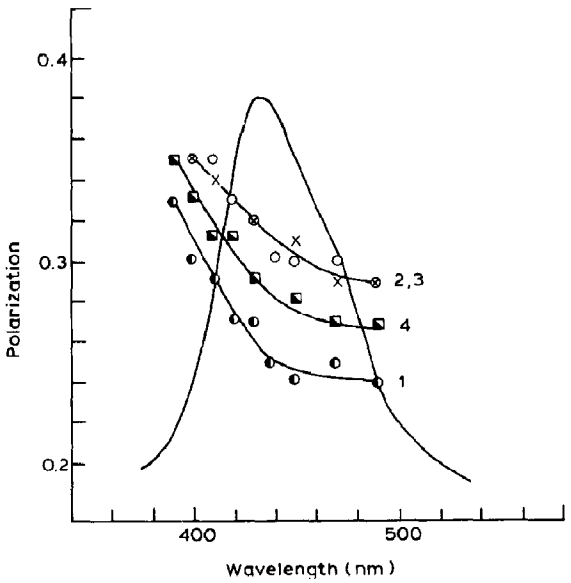

Fig. 7. The dependence of 2,6-TNS fluorescence polarization in phosphatidylcholine vesicles on emission wavelength. Excitation, 360 nm; temperature, 20°C. (1) Without quencher, (2) 2.1×10^{-4} M rhodamine 6G; (3) 1.4×10^{-4} M eosin; (4) 1×10^{-4} M fluorescein. Solid line, emission spectrum.

Water-soluble quenchers that quench predominantly the late states result in an increase in polarization, but their effect is less significant at the short-wave edge of the emission spectrum (fig. 7).

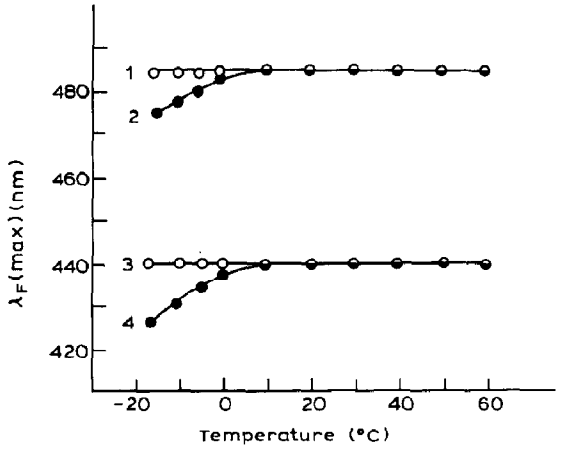

Fig. 8. The dependence of the maxima of the fluorescence spectra λ_F(max) of 1,8-ANS (1,2) and 2,6-TNS (3,4) on temperature. Excitation wavelengths: 410 nm (1), 380 nm (2), 400 nm (3), 360 nm (4).

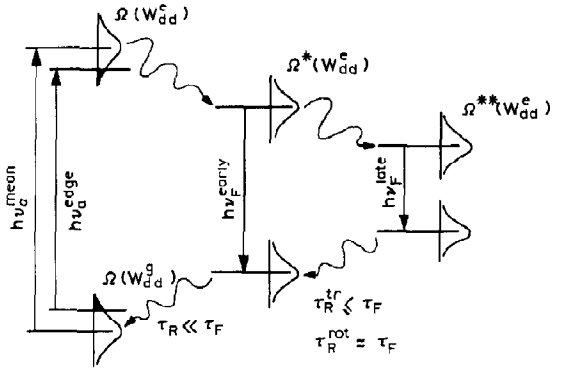

Fig. 9. Diagram of energy levels and transitions and relaxation processes of amphiphilic fluorescence probes in a membrane phospholipid bilayer.

3.5. The edge excitation fluorescence shift is observed at subzero temperature

The dependence of the emission spectra on the excitation wavelength was studied for 2,6-TNS and 1,8-ANS in phosphatidylcholine vesicles at subzero temperatures in the presence of sucrose, serving as a cryoprotector. The results presented in fig. 8 show that the edge excitation fluorescence shift appears on cooling. It is still unclear whether this effect is a direct consequence of the bilayer order transition to the gel state which is known to proceed at -5 to -10°C [34], or if it is due to the combined effect of cooling and the influence of sucrose on the structural dynamics of the bilayer. Nevertheless, under the condition specified one can observe the consequences of slowing down of the dipolar relaxation that becomes comparable with the excited-state lifetime [20]. It should be noted that the process of relaxation is complex and is not described by a single value of τ_R^{dip}. The first observed on cooling is the delayed relaxation of those dipolar groups that are the least perturbed by the interaction with the chromophore [35].

4. Discussion

The kinetics of attaining molecular interaction equilibrium in biological systems is a very important area of research. The fluorescence method offers unique possibilities in these studies. On

excitation the probe molecule drastically changes its chemical and physical properties. It becomes more polar, its dipolar moment alters in magnitude and direction, and it may participate in reactions which could not proceed in the ground state. The high resolution of the method with respect to time allows one to follow directly the transition to a new equilibrium studying pico- and nanosecond kinetics of spectra, as well as other parameters exploiting τ_F as a time marker. However, the structural resolution of the method is not great, and the origin and character of the processes may not always be determined in a single way. The shifts in the time-resolved spectra in general may be due to different phenomena: the structural (dipolar) relaxation [27,36], intramolecular changes of geometric configurations [37], interchange of the nearest-neighbor solvent molecules in mixed solvents [38,39], and excited-state reactions, including proton [40,41] and electron [42] transfer and exiplex formation [43]. Robinson et al. [39], in studies of 1,8-ANS in a liquid water/ethanol mixed solvent, found that the characteristic time for the local solvent relaxation is much shorter than τ_F, but that the interchange of nearest-neighbor solvent molecules lasts longer than τ_F. In inhomogeneous and anisotropic systems, i.e., phospholipid bilayer membranes, anisotropic translational and rotational motions of the probe are possible.

In the present studies an attempt was made to increase the time resolution of the method by applying the analysis of the red-edge excitation fluorescence spectra, indicating the dipolar relaxation as a process of reaching the equilibrium distribution of the dynamic subsites and the direct observations of motions by time-resolved nanosecond spectroscopy. The structural resolution is increased by the application of fluorescence quenchers at different locations. The rotational behavior of the probe was studied following the dependence of the probe emission polarization on temperature and emission wavelength.

The results suggest the following model (fig. 9). The dipolar-orientational equilibrium is established very rapidly, i.e., in the subnanosecond time range. According to Demchenko [19], the environment of the chromophores photoselected by the low-energy quanta $h\nu^{edge}$ is changed during the excitation lifetime. These are the chromophores at the high-energy edge of the distribution on the energy in the ground state $\Omega(W_{dd}^g)$ and the low-energy edge of the distribution in the excitated state $\Omega(W_{dd}^e)$. Emission from these low-energy states results in the long-wave-shifted emission observed in solid and viscous systems. However, similar to liquid solvents, in a phospholipid bilayer the relaxation brings about the new distribution $\Omega^*(W_{dd}^e)$, in which the chromophores excited by the low-energy quanta 'forget about it', and the emission does not depend on the excitation energy. The nanosecond time resolution is not sufficient to observe this process directly; we follow the result only.

There is another process in the nanosecond time range resulting in futher lowering of the emission energy and followed by the nanosecond motion of spectra, complex behavior of emission kinetics and the emission wavelength dependence of polarization. Fluorescence quenchers influence this process differently depending on their location. They quench the early and late emission to a different extent. This suggests that the probe changes its location in the membrane, to move to a more polar environment, the movement being followed by probe rotation resulting in a decrease in polarization.

A number of studies have been published which aimed at establishing the location of 2,6-TNS and 1,8-ANS in the bilayer. Based on X-ray [44] and NMR [45,46] data the charged sulfo group is considered to be located at the level of the phospholipid heads and the hydrophobic heterocycle is directed toward the bilayer and located at the level of the carbonyl groups [3]. The strongest dipole interacting with the chromophore may be the phosphocholine head, the dipolar movement of which is oriented in the plane of the bilayer. Besides, 2,6-TNS and 1,8-ANS are accessible to dipolar molecules of the water of hydration. (The observed significant enhancement of fluorescence intensity on substitution of H_2O for ^2H_2O [47] requires the contact of the probe imino group with water [48].) Thus, the probes studied are significantly influenced by the surrounding dipoles. According to our data dielectric equilibrium with

these groups is reached at very short subnanosecond times, similar to fluid solvents. The nanosecond process brings about a change in interaction energy by several kJ/mol, as may be estimated from time-dependent fluorescence shifts. It does not result in probe dissociation out of the bilayer (the quantum efficiency should decrease manyfold) [22,23]. However, limited movement of the probe along the polarity gradient in the direction normal to the bilayer may be suggested.

The experimental data of this work allow us to estimate the characteristic times of the three different processes of reaching energetic equilibrium of the electronically excited probe molecule with the phospholipid bilayer. The dipolar relaxation that may be described by the relaxation time τ_R^{dip} results in equilibration of the surrounding dipoles with respect to the chromophore and formation of the new equilibrium in the distribution of these groups according to interaction energy. The translational relaxation (relaxation time τ_R^{tr}) results in probe translational movement and attainment of the equilibrium position of the probe in the area of the membrane of definite polarity. And, finally, the rotational relaxation time τ_R^{rot} describes the orientational movements (rotations) of the probe in the bilayer. Under the conditions studied the following correlations hold:

$$\tau_R^{dip} \ll \tau_F;\ \tau_R^{tr} \leqslant \tau_F;\ \tau_R^{rot} \approx \tau_F$$

It is important that similar results are obtained for the two distinct probes, 2,6-TNS and 1,8-ANS, structural analogs with different electronic structures and dimensions of the molecule. The dynamic properties of the polar region of the lipid bilayer appear not to be significantly influenced by the chemical composition and the phase state of the acyl side chains [13,14]. It is natural to suggest that the processes defined above may describe the phenomenon of reaching equilibrium not only of informative fluorescent probes, but also of 'silent' amphiphilic molecules in their interaction with the phospholipid bilayer membrane.

Acknowledgements

The authors are grateful to Research Workers of the Institute of Physics of the Byelorussian Academy of Sciences (Minsk), Professor A.N. Rubinov, Drs. V.I. Tomin and N.A. Nemkovich for profitable discussion, and V.B. Pavlenko for assistance in time-resolved spectroscopic studies.

References

1 L. Brand and J.R. Gohlike, Annu. Rev. Biochem. 41 (1972) 843.
2 A. Azzi, Q. Rev. Biophys. 8 (1975) 237.
3 J. Slavik, Biochim. Biophys. Acta 694 (1982) 1.
4 M.T. Flanagan and S.C. Ainsworth, Biochim. Biophys. Acta 168 (1968) 16.
5 C. Huang and J.P. Charlton, Biochemistry 11 (1972) 735.
6 D.H. Haynes and H. Staerk, J. Membrane Biol. 17 (1974) 313.
7 G.K. Radda and D.S. Smith, Biochim. Biophys. Acta 318 (1973) 197.
8 Yu.A. Vladimirov and G.E. Dobretsov, Fluorescent probes in the study of biological membranes (Nauka, Moscow, 1980) p. 320.
9 J.H. Easter and L. Brand, Biochim. Biophys. Res. Commun. 52 (1973) 1086.
10 R.P. DeToma, J.H. Easter and L. Brand, J. Am. Chem. Soc. 98 (1976) 5001.
11 J.H. Easter, R.P. DeToma and L. Brand, Biochim. Biophys. Acta 508 (1978) 27.
12 J.H. Easter, R.F. DeToma and L. Brand, Biophys. J. 16 (1976) 571.
13 J.R. Lakowicz and D. Hogen, Biochemistry 20 (1981) 1366.
14 J.R. Lakowicz, R.B. Thompson and H. Cherek, Biochim. Biophys. Acta 734 (1983) 295.
15 J.C.W. Shepherd and G. Buldt, Biochim. Biophys. Acta 514 (1978) 83.
16 J. Seeling, L. Tamm, L. Hymel and S.F. Flescher, Biochemistry 20 (1981) 3922.
17 H.U. Gally, W. Niederberger and J. Seeling, Biochemistry 14 (1975) 3647.
18 P.L. Yeagle, W.C. Hutton, C.-H. Huang and R.B. Martin, Proc. Natl. Acad. Sci U.S.A. 72 (1975) 3477.
19 A.P. Demchenko, Biophys. Chem. 15 (1982) 101.
20 A.P. Demchenko, J. Mol. Struct. 114 (1984) 45.
21 D.M. Small and M.C. Bourger, Biochim. Biophys. Acta 125 (1966) 563.
22 W.O. McClure and G.M. Edelman, Biochemistry 5 (1966) 1908.
23 D.C. Turner and L. Brand, Biochemistry 7 (1968) 3381.
24 R.F. Chen and R.L. Bowman, Science 147 (1965) 729.
25 A.N. Rubinov and V.I. Tomin, Opt. Spectrosc. (U.S.S.R.) 30 (1971) 275.
26 W.C. Galley and R.M. Purkey, Proc. Natl. Acad. Sci U.S.A. 67 (1970) 1116.
27 A.N. Rubinov, V.I. Tomin and B.A. Bushuk, J. Lumin. 26 (1982) 377.
28 R.B. Macgregor and G. Weber, Ann. N.Y. Acad. Sci, 366 (1981) 140.

29 G.G. Bakhshiev, Spectrocopy of intermolecular interactions (Nauka, Leningrad, 1972) p. 263.
30 K.P. Ghiggino, A.G. Lee, S.R. Meech, D.V. O'Connor and D. Phillips, Biochemistry 20 (1981) 5381.
31 V.T. Koyava, V.I. Popechits and A.M. Sarjevsky, Opt. Spectrosc. (U.S.S.R.) 48 (1980) 896.
32 I.M. Gulis and A.I. Komyak, J. Appl. Spectrosc. (U.S.S.R.) 32 (1980) 897.
33 S.R. Anderson and G. Weber, Biochemistry 8 (1969) 317.
34 D.F.H. Wallach, S.P. Verma and J. Fookson, Biochim. Biophys. Acta 559 (1979) 153.
35 V.S. Pavlovich, L.G. Pikulik and P.P. Petrushkevich, J. Appl. Spectroc. (U.S.S.R.) 31 (1979) 998.
36 W.R. Ware, S.K. Lee, G.J. Brant and P.P. Chow, J. Chem. Phys. 54 (1971) 4729.
37 Yu.T. Mazurenko, V.C. Udaltsov and A.C. Cherkasov, Opt. Spectrosc. (U.S.S.R.) 46 (1979) 696.
38 Yu.T. Mazurenko and V.C. Udaltsov, Opt. Spectrosc. (U.S.S.R.) 45 (1978) 255.
39 G.W. Robinson, R.J. Robbins, G.R. Fleming, J.M. Morris, A.E.W. Knight and R.J.S. Morrison, J. Am. Chem. Soc. 100 (1978) 7145.
40 Yu.T. Mazurenko and V.C. Udaltsov, Opt. Spectrosc. (U.S.S.R.) 49 (1980) 304.
41 L. Brand, J.B.A. Ross and W.R. Laws, Ann. N.Y. Acad. Sci. 366 (1981) 197.
42 M.A. El-Bayoumi, J. Phys. Chem. 80 (1979) 2259.
43 R.P. DeToma and L. Brand, Chem. Phys. Lett. 47 (1977) 231.
44 W. Lesslauer, J.E. Cain and J.K. Blasie, Proc. Natl. Acad. Sci U.S.A. 69 (1972) 1499.
45 F. Podo, Biochimie 57 (1975) 461.
46 F. Podo and J.K. Blasie, Proc. Natl. Acad. Sci U.S.A. 74 (1977) 1032.
47 G.K. Radda and J. Vanderkooi, Biochim. Biophys. Acta 265 (1972) 509.
48 L. Stryer, J. Am. Chem. Soc. 88 (1966) 5708.